Commun Nonlinear Sci Numer Simulat 44 (2017) 292–303

Contents lists available at ScienceDirect

Commun Nonlinear Sci Numer Simulat

journal homepage: www.elsevier.com/locate/cnsns

Research paper

A comparison study on stages of sleep: Quantifying multiscale complexity using higher moments on coarse-graining

Wenbin Shi[a,b], Pengjian Shang[a], Yan Ma[b], Shuchen Sun[c], Chien-Hung Yeh[d,e,*]

[a] School of Science, Beijing Jiaotong University, Beijing 100044, P R of China
[b] Division of Interdisciplinary Medicine and Biotechnology, Department of Medicine, Beth Israel Deaconess Medical Center, Harvard Medical School, Boston, MA 02215, USA
[c] Department of Otolaryngology and South Campus Sleep Center, Guang'anmen Hospital, China Academy of Chinese Medical Sciences, Beijing 100053, P R of China
[d] Department of Neurology, Chang Gung Memorial Hospital and University, Taoyuan City 333, Taiwan
[e] Division of Sleep and Circadian Disorders, Brigham and Women's Hospital, Harvard Medical School, 221 Longwood Avenue, Boston, MA 02115, USA

ARTICLE INFO

Article history:
Received 15 February 2016
Revised 20 August 2016
Accepted 25 August 2016
Available online 28 August 2016

Keywords:
Multiscale entropy
Higher moments coarse-graining
EEG
Sleep stages

ABSTRACT

It is of great interests in identifying dynamical properties of human sleep signals using electroencephalographic (EEG) measures. Multiscale entropy (MSE) is effective in quantifying the degree of unpredictability of time series in different time scales. To understand the superior coarse-graining approach for the EEG analysis, we therefor use different moments to coarse-grain a time series, and examine their volatility as well as the effectiveness in quantifying the complexities of sleep EEG in different sleep stages. Both the simulated signals (logistic map) and the EEGs with different sleep stages are calculated and compared using three types of coarse-graining procedure: including MSE_{μ} (mean), MSE_{σ^2} (variance) and MSE_{skew} (skewness). The simulated results show that the generalized MSE (including MSE_{σ^2} and MSE_{skew}) can identify the differences in chaotic more easily with less fluctuation of entropy values in different time scales. As for the analysis of human sleep EEG, we find: (1) at small scales (<0.04 s), the entropy is higher during wakefulness and increasing time scales. (2) At large scales (0.25 s–2 s) in contrast, entropy is higher during deep sleep and lower with increasing time scales.

1. Introduction

It is well-known that a high-quality sleep can ensure the well-function in our daily lives, such as mental health, creative ability and working performance. Insufficient or ineffective sleep can cause daytime sleepiness, irritability, emotional distress, depressive or anxious mood, or even increased accident rates. In clinical, a variety of sleep measures are used in the identification and classification of sleep quality [1–4]. Unlike the Epworth Sleepiness Scale [5] which is subjective, polysomnographic (PSG), a multi-parametric test, is frequently used in sleep medicine and a popular diagnostic tool in the study of sleep. The PSG includes a comprehensive recording of the physiological changes, including electroencephalogram (EEG), electrooculogram (EOG), chin electromyogram (EMG), electrocardiogram (ECG), oxygen saturation (SpO2), and respiration (Resp.) [6]. Among them, EEG raises the most attention due to its representation as well as the rich information in

* Corresponding author.
E-mail address: nzdiw1120@gmail.com (C.-H. Yeh).

http://dx.doi.org/10.1016/j.cnsns.2016.08.019

brain activities [7]. In 1968, Rechtschaffen & Kales (R&K) [8] classified sleep/wake into three types of stages (epoch length = 30 s): Awake, non-rapid eye movement (including N-REM stage 1, N-REM stage 2, N-REM stage 3), and rapid eye movement (REM). Although the exact mechanisms of sleep, learning, and memory are not entirely understood, researchers believe that specific features of EEGs during different sleep stages are associated with the formation of particular types of memory. In particular, the relationship between the consolidation of different types of memories and the various sleep stages has raised a great deal of attention in recent years. Thus, it is essential to understand the changes in the sleep architecture during sleep cycles, numerous methods were therefore proposed in detecting the EEG features in each sleep stage in the last decades. For example, wavelet packet coefficients and artificial neural networks were deployed to classify sleep stages [9]; detrended fluctuation analysis was applied to analyze the fluctuation of EEG features in sleep apnea patients [10], the non-linear parameters: correlation dimension, fractal dimension, largest Lyapunov entropy, approximate entropy, Hurst exponent, phase space plot and recurrence plots were compared in quantifying the cortical function at different sleep stages [11].

However, it is still remains a challenge in identifying the sleep stages in sleep research society due to the highly complicated waveform of EEG; that is, both the amplitudes and frequencies are modulating in nonlinear and nonstationary patterns. Generally, EEG comprises the waves and events as: Delta waves (0.5–4 Hz), Theta waves (4–8 Hz), Alpha waves (8–13 Hz), Beta waves (13–35 Hz), Sleep spindles (12–14 Hz), and *K*-complexes (0.5–1.5 Hz) [6]. The complexity and changeability of EEG therefore bring about the necessity of applying dynamical and multiple time scales approaches in extracting the characteristics of sleep EEG, and let the temporal structure to tell its own story. To extract features in EEG signals, different methods are used in the calculation, such as standard deviation [12], power density [13], fractals [14] and information entropy [15–17]. Other than the above mentioned methods, sample entropy is excellent in quantifying the temporal structure of complex systems [18,19]. The MSE method [20], employing sample entropy as a measure in quantifying the degree of unpredictability of time series in different time scales, can be particularly informative and straightforward in describing the dynamic changes of physiological status. The application scopes of this method involve quantifying brain signal variability [15], illustrating the feasibility and well performance in the brain death diagnosis [21] and so on. Besides, Bell et al. [22] also showed that MSE can provide sensitive measures in nonlinear and dynamical systems and evaluate homeopathic remedy effects on human sleep EEG patterns.

Coarse-graining, an essential operation in the realization of MSE, is a procedure that obtains a new series using the mean value in each non-overlapping segments of equal length as the new variable. An interesting question is whether we will discard important information in using the first moment (mean value) in deriving copies of the original signal in different time scales. In 2015, Costa et al. used variance in the coarse-graining procedure with its application to heart beat time series [23]. However, the availability of using skewness in coarse-graining is remained unvalidated, nor its possibility in telling the distinction of the sleep stages. In our study, we compare the MSE results using multiscale entropy with generalization to higher moments (MSE_n) to coarse-grain the original time series. The previously MSE method is represented as MSE_μ, here μ stands for the first moment (mean). On the other hand, we also study the performances of MSE using second moment MSE_{σ^2} (variance) and third moment MSE_{Skew} (skewness). In order to examine the effectiveness and reliabilities in identifying the complexities between the three coarse-graining approaches, the logistic map, a family of nonlinear dynamical series with different degree of chaotic behavior is analyzed at first. After that, we apply MSE_n to identify the differences of temporal structure with different time scales into EEG derivation in healthy human during sleep.

In Section 2, we elaborate the detail methodology in quantifying multiscale entropy with higher moments. After the verification of the effectiveness in different methods using simulated signals in Section 3.1. Section 3.2 describes the data collection and the experiment protocols. The MSE_n results of the real data are shown in Section 3.3. At last, Section 4 concludes our findings.

2. Methodology

2.1. Sample entropy

Sample entropy (SampEn) quantifies the regularity of a time series. Mathematically, the procedure goes as follows.

For a time series $\{x_1, x_2, \ldots, x_N\}$, with the data length N, $N-m+1$ template vectors $\mathbf{x}_m(i) = (x_i, x_{i+1}, \ldots, x_{i+m-1})$ with $\{i|1 \le i \le N-m+1\}$ are considered, where m is the embedding dimension, and r stands for the tolerance for the accepting matches. The distance between each pair of vectors is defined as the maximum difference between the two vectors

$$d[\mathbf{x}_m(i), \mathbf{x}_m(j)] = \max |x_{i+k} - x_{j+k}| : \ 0 \le k \le m-1 \tag{1}$$

Suppose B_i is the number of pairs with their distances smaller than r between $\mathbf{x}_m(i)$ and $\mathbf{x}_m(j)$, where $i \neq j$; and A_i is the number of pairs with their distances smaller than r between $\mathbf{x}_{m+1}(i)$ and $\mathbf{x}_{m+1}(j)$, where $i \neq j$. The probability that $\mathbf{x}_m(j)$ is within r of $\mathbf{x}_m(i)$ is

$$B_i^m(r) = \frac{B_i}{N-m-1}, \tag{2}$$

and the density is

$$B^m(r) = \frac{1}{N-m} \sum_{i=1}^{N-m} B_i^m(r). \tag{3}$$

Similarly, $A_i^m(r) = \frac{A_i}{N-m-1}$ and $A^m(r) = \frac{1}{N-m}\sum_{i=1}^{N-m} A_i^m(r)$ represent the probability and density for $\mathbf{x}_{m+1}(j)$ is within r of $\mathbf{x}_{m+1}(i)$, respectively. The total number of template matches in a m-dimensional ((m + 1)-dimensional) state space within a tolerance r can be calculated as

$$B(r) = \frac{1}{2}(N-m-1)(N-m)B^m(r), \tag{4}$$

and

$$A(r) = \frac{1}{2}(N-m-1)(N-m)A^m(r). \tag{5}$$

Finally, sample entropy is defined by the following formula

$$SampEn(m, r, N) = -\log\left(\frac{A(r)}{B(r)}\right) \tag{6}$$

Hence, the sample entropy is the negative natural logarithm of the conditional probability that a dataset of length N, having repeated itself for m points within a tolerance r, will also repeat itself for $m+1$ points, excluding self-matches [24].

2.2. Generalized multiscale entropy

We introduce the generalization of multiscale entropy MSE_n, where the subscript denotes the moment used to coarse-grain a time series. The traditional MSE is represented as MSE_μ, where μ refers to the mean (first moment).

For a given time series, $\mathbf{x} = \{x_1, x_2, \cdots, x_N\}$, we divide it into non-overlapping segments with equal length τ. The coarse-grained time series $\{\mathbf{y}^{(\tau)}\}$ at scale τ is then derived as

$$\mathbf{y}_j^{(\tau)} = \frac{1}{\tau}\sum_{i=(j-1)\tau+1}^{j\tau} x_i, \quad \text{for the first moment} \tag{7}$$

$$\mathbf{y}_j^{(\tau)} = \frac{1}{\tau-1}\sum_{i=(j-1)\tau+1}^{j\tau} (x_i - \bar{x}_j)^2, \quad \text{for the second moment} \tag{8}$$

$$\mathbf{y}_j^{(\tau)} = \frac{1}{\tau}\sum_{i=(j-1)\tau+1}^{j\tau} (x_i - \bar{x}_j)^3, \quad \text{for the third moment} \tag{9}$$

$$\cdots$$

$$\mathbf{y}_j^{(\tau)} = \frac{1}{\tau}\sum_{i=(j-1)\tau+1}^{j\tau} (x_i - \bar{x}_j)^n, \quad \text{for the selected moment } n. \tag{10}$$

In Eq. (10), τ denotes the scale factor and $1 \le j \le N/\tau$. Fig. 1 shows the schematic diagram of the coarse-graining procedure for MSE_n. In our study, we compare the results of the first three moments: MSE_μ (Eq. (7)), MSE_{σ^2} (Eq. (8)) and MSE_{Skew} (Eq. (9)), that stand for mean, variance and skewness, respectively. The selections are based on their clear definition in mathematics, and hence it will be easier to be comprehended [25,26]. Note that only MSE_μ can we coarse-grain in $\tau = 1$, which the coarse-graining series is still remained as the original time series. Similarly, the scale is starting from 2 for MSE_{σ^2}, and 3 for MSE_{Skew}. Besides, the parameters m and r is chosen based on the standard proposed by Lake et al. [27], a reporting solution that can calculate the confidence interval of SampEn.

3. Results and discussions

3.1. Numerical simulation

To examine the effectiveness of MSE_n method, we use a chaotic deterministic signal (logistic map), a polynomial mapping that widely cited in the publications related to complex, chaotic and dynamical systems [28–31], as our simulated signals. Mathematically, the logistic map is a recurrence relation as

$$x_{n+1} = Rx_n(1 - x_n), \tag{11}$$

where x_n is a number between zero and one that represents the ratio of existing population to the maximum possible population. The parameter R controls the behaviour of the samples. For example, the samples either converge to a single fixed point ($R \le 3$) or oscillate between few values ($3 < R < 3.54$) for smaller R. For larger R, the variation of the samples is increasing with more complex behavior emerging. In our study, we use 10000 samples of data length to ensure a reliable

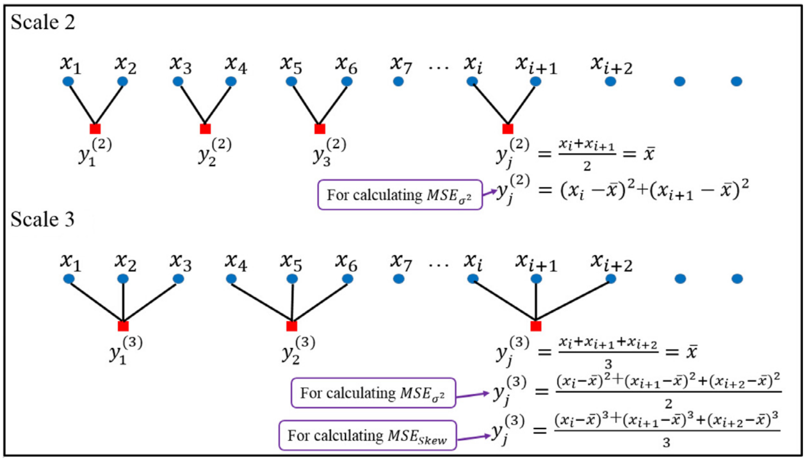

Fig. 1. Schematic diagram of the generalized coarse-graining procedure. For scale 2 ($\tau = 2$), MSE_{μ} and MSE_{σ^2} can be calculated; as for scale 3 ($\tau = 3$), MSE_{μ} and MSE_{σ^2} and MSE_{Skew} can all be obtained, where $\bar{x}$ is the mean of values in the jth window.

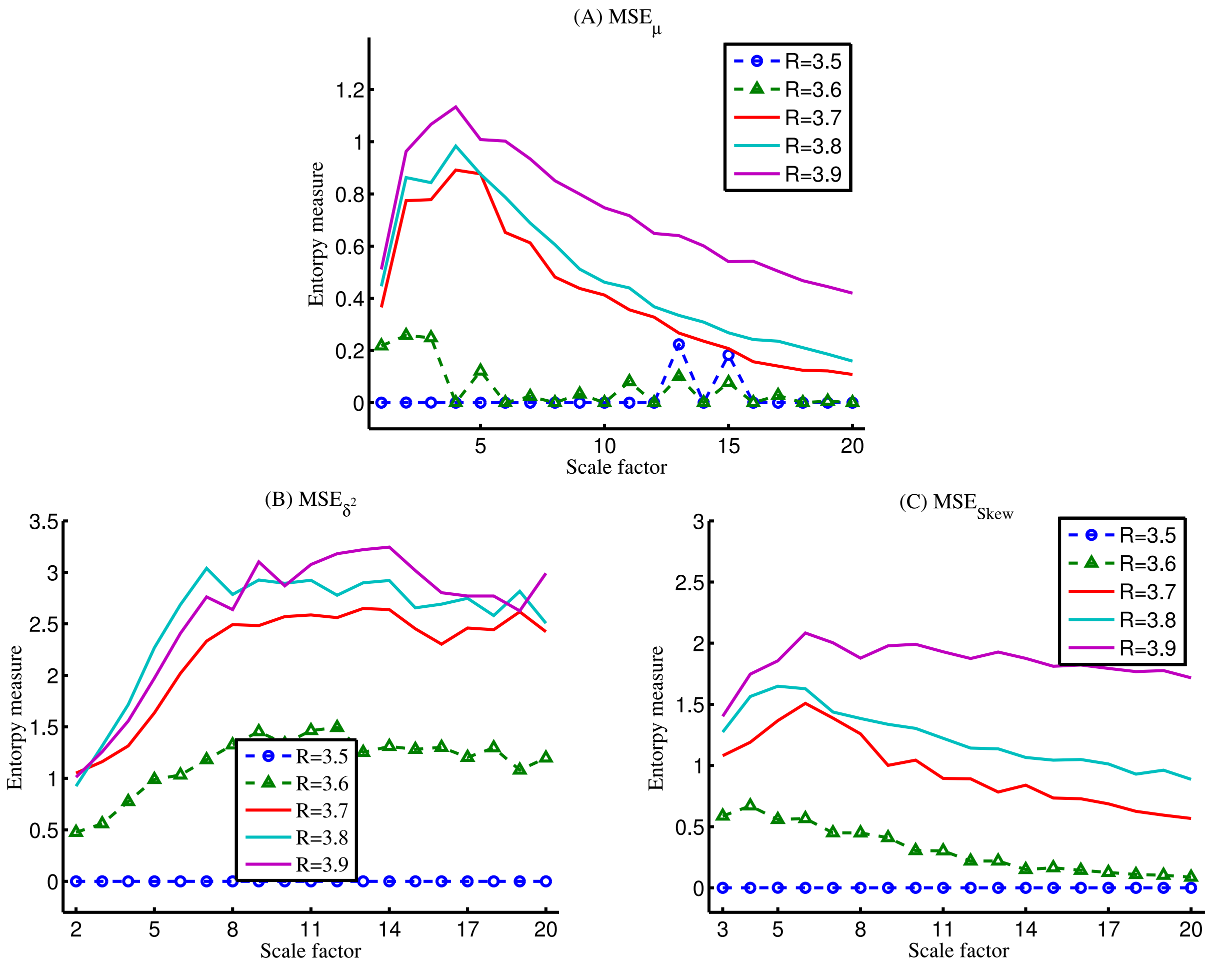

Fig. 2. Comparison results of (A) MSE_{μ} (B) MSE_{δ^2} and (C) MSE_{Skew} ($m = 2$ and $r = 0.15$ of the original time series' standard deviations) for logistic map ($N = 10000$ and $R = [3.5, 3.9]$ with step size = 0.1.

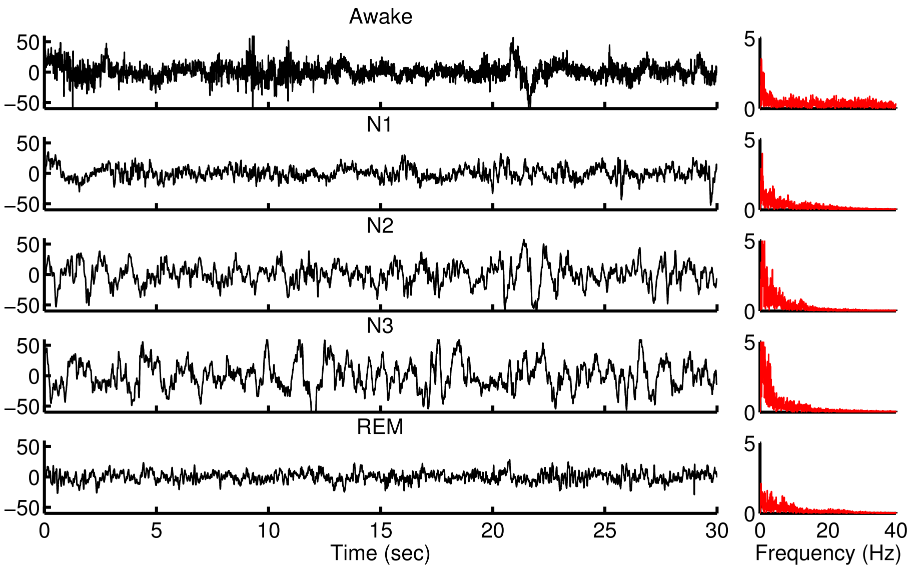

Fig. 3. Oscillation and spectrum of different sleep stages. A wide range of frequencies can be found during the wakefulness, possible features are theta, alpha, and beta activity. N1 is scored when the epoch is characterized with less than 50% alpha activity, and it is a transitional stage between the wakefulness and sleep. N2 is characterized by wave patterns sleep spindles (12–14 Hz) and K-complexes (a sharp negative wave followed by a slower positive one) and the absence of slow waves. With the high-voltage slow-wave activity gradually increasing to more than 20% of an epoch, N3 stage or deep sleep stage is identified. REM stage shows low voltage in low frequency (compared to the N-REM stage) and multiple frequencies (mainly theta and alpha), saw-tooth waveform is often appearing during this stage.

MSE result [32] with parameter values R ranging from 3.5 to 3.9 (step size = 0.1). $R = 3.5$ is a special case with periodic pattern, while the other cases ($R \neq 3.5$) show chaotic dynamics.

The MSE_n results of the simulated signals are shown in Fig. 2. Generally, the entropy measures are decreasing with the reduction in complexity (lower R value) of the logistic map (see Fig. 2 (A-C)). Briefly, the simulated results show that: (1) When $R = 3.5$, the complete predictability of the volatility behavior supposed to reduce the entropy measure into zero. Unlike MSE_{δ^2} and MSE_{Skew} that all the entropy measures can maintain as zero in all time scales (see Fig. 2 (B and C)), two of 20 scales (13 and 15) do not preserve as zero with their values even larger than the case $R = 3.6$ when using MSE_{μ} (see Fig. 2 (A)). (2) Complex performance supposed to appear (entropy measure > 0) when $R = 3.6$. However, the entropy measures quantified by MSE_{μ} are severely mixed with the completely predictable case ($R = 3.5$) in a wide range of time scales (see Fig. 2 (A)). In contrast, there are clear differences in entropy measures when using MSE_n with higher moments, especially in MSE_{δ^2} (see Fig. 2 (B)). (3) When using MSE_{μ} and MSE_{Skew}, the entropy measure markedly increases on small time scales and then gradually decreases for R value larger than 3.7. However, the entropy measure quantified by MSE_{δ^2} increases on small time scales and then stabilizes to a relatively constant value. By examining the performances of the deterministic signals, we confirm that MSE_{Skew} is superior to the other two moments both in its validity in different R value and clear variation in different time scales.

3.2. Data collection

Four healthy male subjects (27-38 yrs with mean age 32.0 ± 4.6yrs) were recruited. Participants were requested to sleep in a standard sleep lab following an all-night Polysomnography (PSG, Compumedics, Australia). All of the research protocols followed the guideline of the American Academy of Sleep Medicine (AASM). Recommended recordings include: 6-channel EEG montage, bilateral EOG, chin surface and bilateral anterior tibialis surface EMG, Resp. effort (chest and abdominal excursion), nasal pressure and airflow, snoring sensor, SpO2, ECG and body position. At least one registered polysomnographic technologist was on the spot throughout the night during the sleep study. PSGs were scored based on 30 s epochs during the night, and were reviewed by experienced sleep specialists. The sampling frequency of EEG signals (channel C4-M1) in our study is 512 Hz.

Fig. 3 shows the raw data of EEG signals in sleep stages including Awake, N-REM stage 1 (N1), N-REM stage 2 (N2), N-REM stage 3 (N3), and REM stage recorded on a healthy subject (Subject 3). Briefly, N1 is the stage between wakefulness and sleep, and the period of transition from relatively unsynchronized beta (12–30 Hz) and gamma (25–100 Hz) brain waves, which is the normal range for the Awake state, to more synchronized but slower alpha waves (8–13 Hz), and then to theta waves (4–7 Hz). It is difficult to pinpoint the actual point of sleep onset (falling asleep), as the process is a continuum as brain wave activity gradually slows down. During N1, hypnagogic jerks are commonly happened. N2, the first unequivocal stage of sleep, is mainly in the theta waves (4–7 Hz) and accompanied with sleep spindles (12–14 Hz) or K-complexes. N3

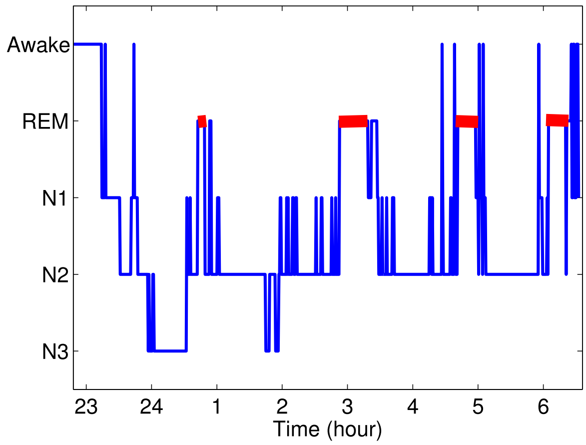

Fig. 4. The annotation of sleep stages in a single night in one of the four subjects (Subject 3).

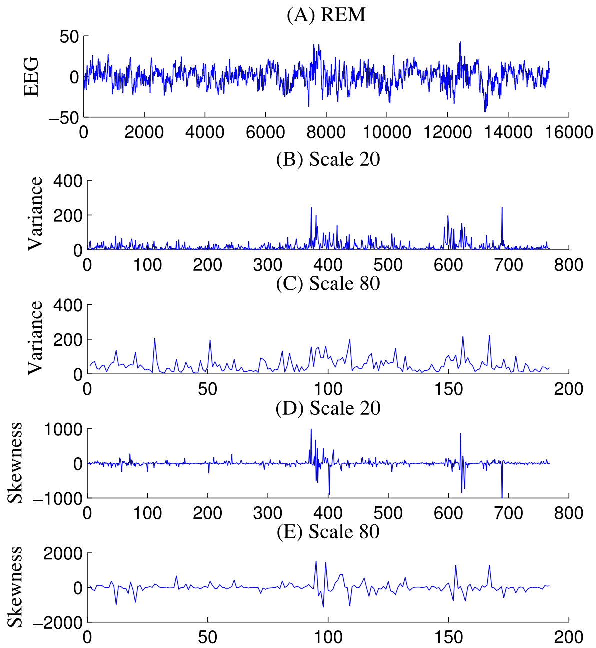

Fig. 5. The comparison of coarse-grained time series in different time scale. (A) is an epoch in REM stage, and both the variance (B,C) and skewness (D,E) derived coarse-grained time series show higher frequency at scales 20 (B,D) than scale 80 (C,E).In the meanwhile, the oscillation is larger when using higher moments in the coarse-graining procedure.

is dominated by delta waves (0.5–4 Hz). REM stage is characterized by the rapid and random eye movement, high frequency (including theta, alpha and even beta) waves similar to the wakefulness, and dreaming is mainly occurred during the REM sleep. During the sleep, the balance of sympathetic and vagal will modulate in different sleep stages; briefly, the vagal tone is stronger during deep sleep as compared to the light sleep, and vice versa. Fig. 4 shows a typical case of an all-night sleep. The normal sleep cycles in a healthy adult start from N-REM sleep, and REM sleep will not appear until 80 min or longer thereafter. N-REM and REM sleep will alternate with their weight in sleep cycles changed through the night (sleep cycle $\sim$ 90 min) [33], and N3 appears more often in the first three sleep cycles which is related to the initiation of sleep and the length of time awake [33]. REM sleep, associates with dreaming, usually predominates in the last three sleep cycles. In Fig. 4, segments with REM sleep are highlighted in red.

3.3. MSE_n results of human sleep EEG

The distribution of sleep epochs of the four subjects is shown in Table 1, and the movement group represents the artificial epochs caused by body movement. To compare the effectiveness of MSE_n in differentiating sleep stages at different time scales, we first focus on the complexities at small scales ($\leq$20). For each subject, the mean entropy measure is calculated

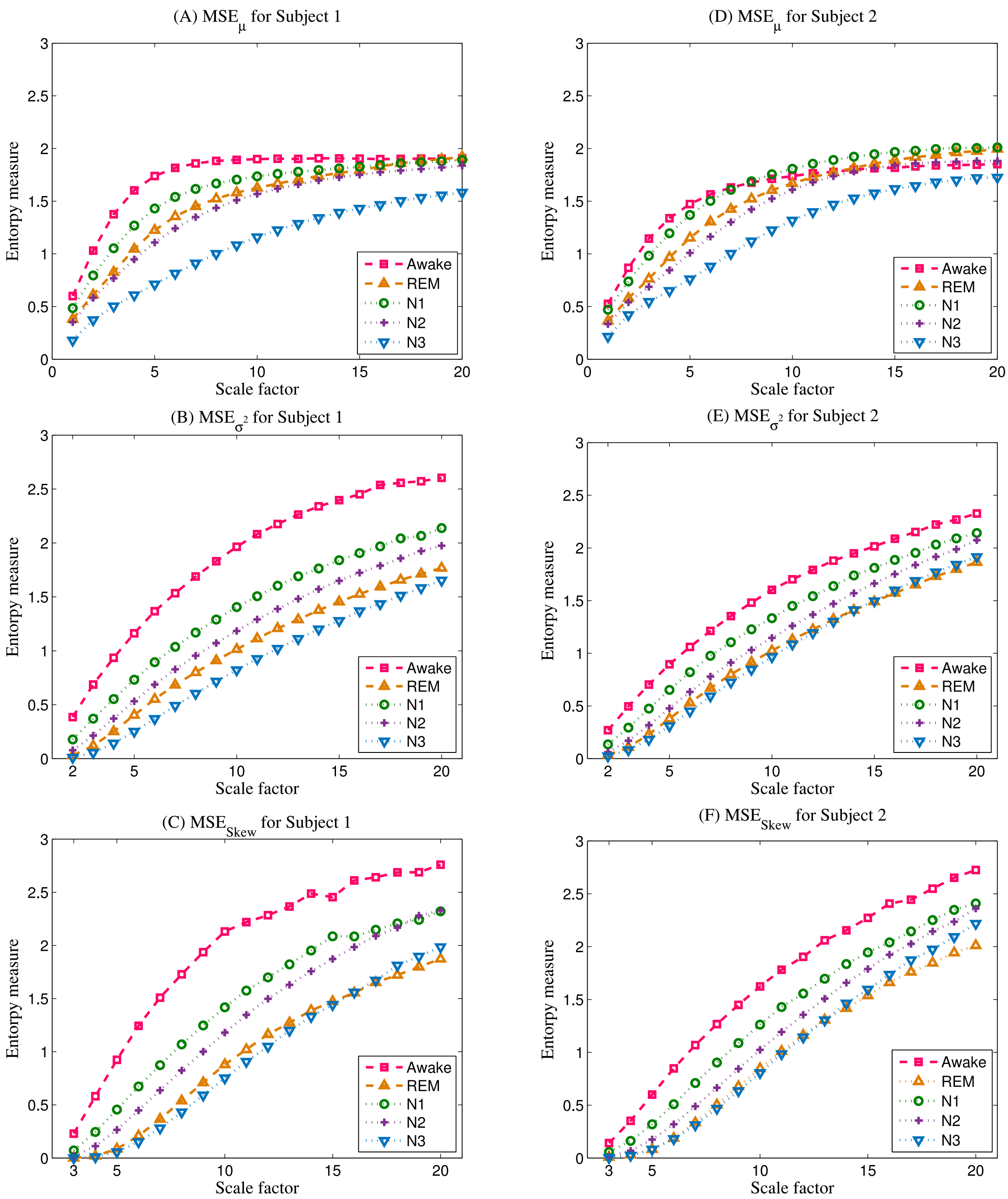

Fig. 6. MSE$_n$ results of healthy human sleep EEG during the five sleep stages. (A), (D), (G), (J) are MSE$_\mu$ results ($m = 2$ and $r = 0.15$SD). (B), (E), (H), (K) show the MSE$_{\sigma^2}$ results ($m = 2$ and $r = 0.5$SD). (C), (F), (I), (L) are MSE$_{Skew}$ results ($m = 2$ and $r = 5$SD).

Table 1
The percentage of stages among the total epochs (epoch length = 30 *s*).

Sleep stages	Awake	REM	N1	N2	N3	Movement
Subject 1	6.71%	15.47%	11.63%	50.96%	8.03%	7.19%
Subject 2	4.34%	22.04%	13.01%	46.25%	5.69%	8.67%
Subject 3	33.86%	11.48%	11.36%	23.75%	13.64%	5.91%
Subject 4	16.55%	9.16%	15.50%	42.77%	9.89%	6.14%

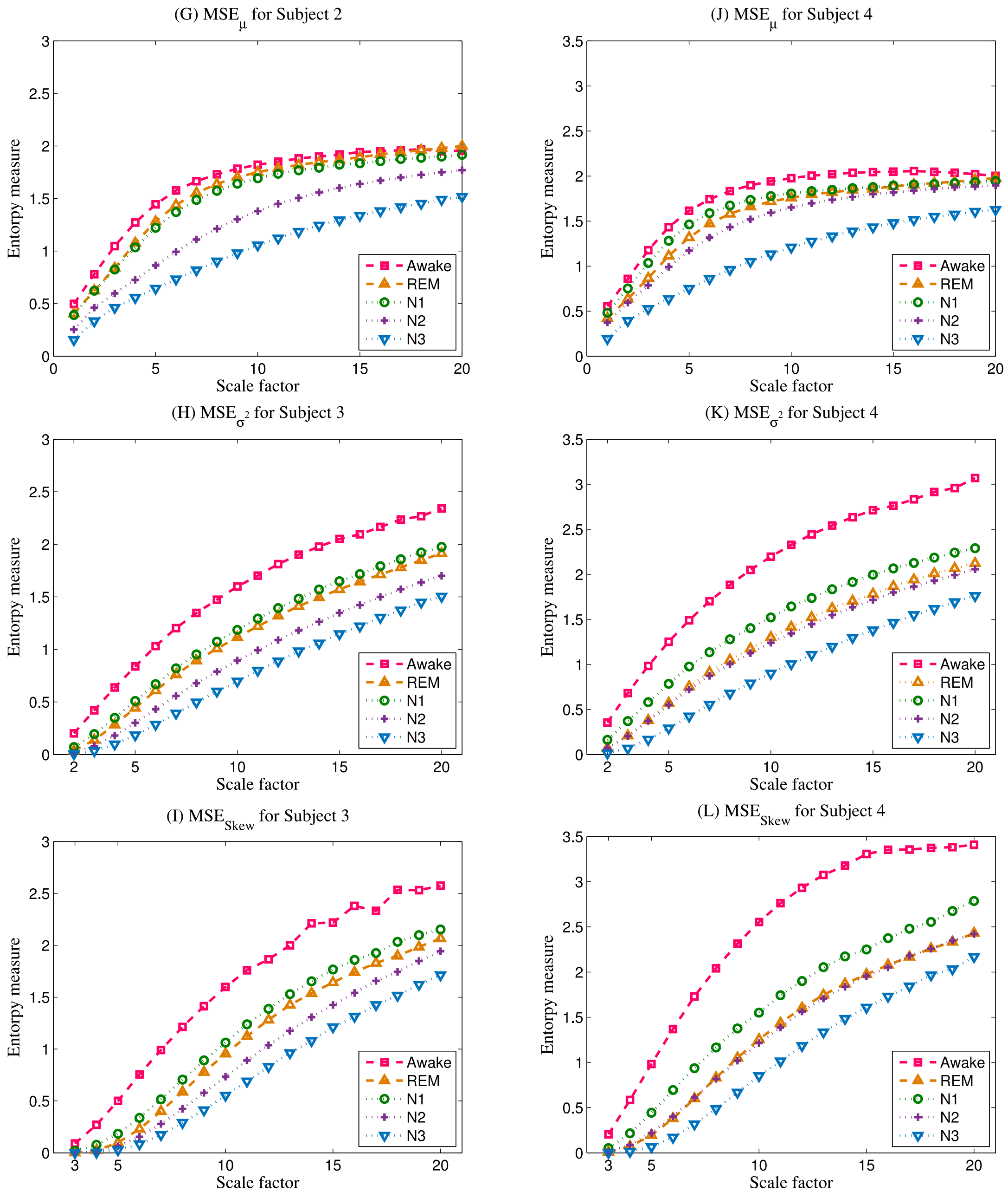

Fig. 6. Continued

for each sleep stage as

$$MSE_n(\Theta) = \frac{\sum_{\theta \in \Theta} MSE_n(\theta)}{\sharp(\Theta)}, \tag{12}$$

where Θ represents the stage of sleep, θ is the epoch of the sleep stage identified as Θ, and $\sharp$ is the cardinality of Θ: the number of epoches identified as stage Θ.

For MSE$_\mu$, we use $m = 2$ and $r = 0.15$SD (the original time series' standard deviations) [32]. Unlike MSE$_\mu$, different parameters ($m = 2$ and $r = 0.5$SD) are selected for the analysis of MSE$_{\sigma^2}$; similarly, we use $m = 2$ and $r = 5$SD in calculating MSE$_{Skew}$. The selections of the parameters are based on the principle proposed by Lake et al. [27]. Briefly, the differences in the choice of the r values should be adjusted according to the magnitude of coarse-grained time series. Since the values of the variance and skewness coarse-grained time series are much larger than those of the mean coarse-grained time series, larger r values should be applied to ensure sufficient matching templates that can be appropriately identified. Fig. 5 visualize

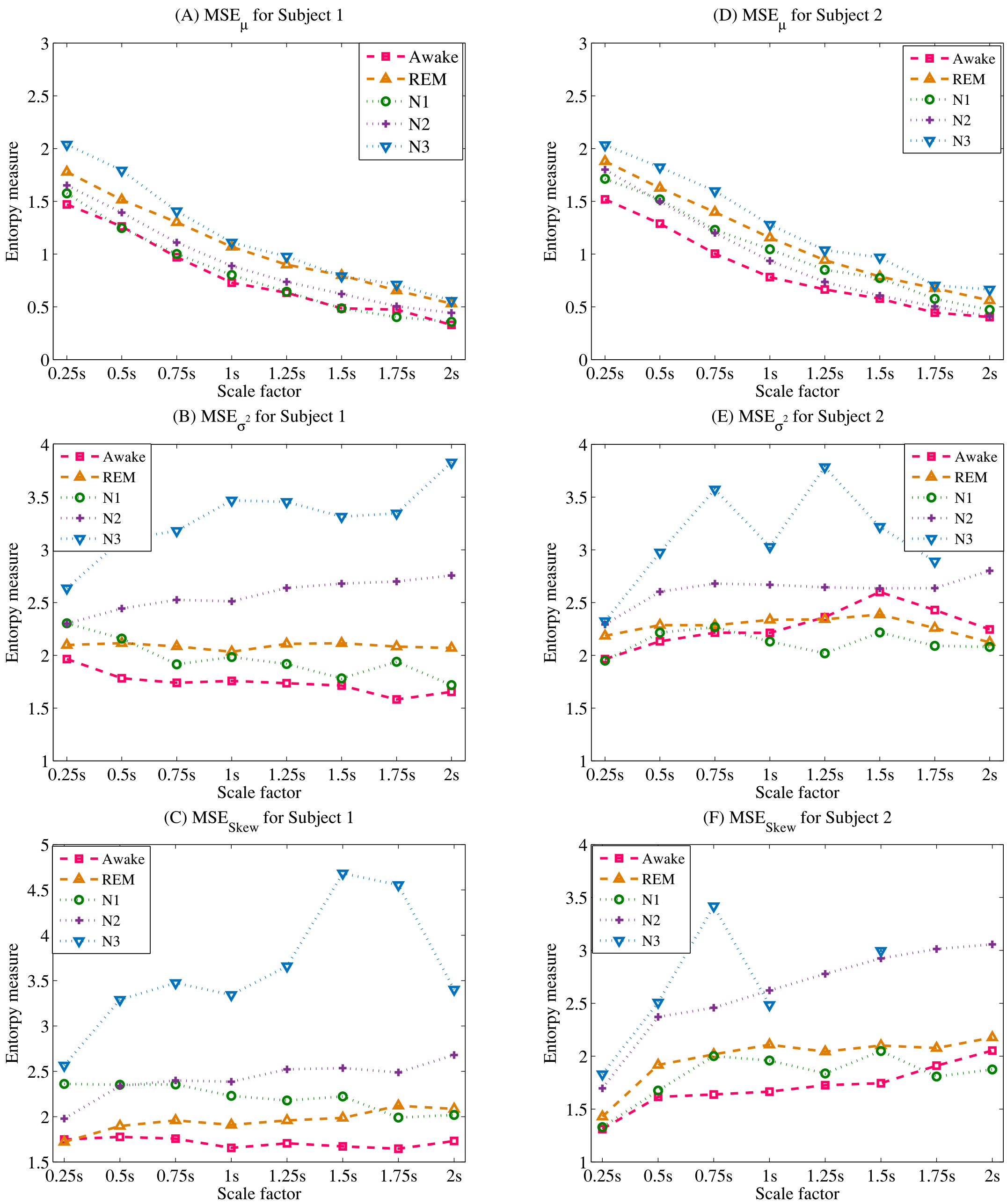

Fig. 7. MSE$_n$ results of different sleep stages at large scales (0.25 s–2 s). For each subjects, Figure (A), (D), (G), (J) are MSE$_\mu$ results ($r = 0.15$SD); MSE$_{\sigma^2}$ ($r = 0.5$SD) results are shown in figure (B), (E), (H), (K); and MSE$_{Skew}$ ($r = 5$SD) results are shown in figure (C), (F), (I), (L). The choice of parameter r is based on the principle proposed by Lake et al. [27] (see details in Section 3.3).

the differences in MSE$_n$ (variance and skewness) at different time scales (20 and 80): Fig. 5(A) shows an epoch identified as REM stage (Subject 3), it is clearly shown that the amplitude variation of the coarse-graining series using variance Fig. 5(B) and (C)) is much smaller than the one using skewness Fig. 5(D) and (E)), therefore it is a necessity in adjusting parameter r according to the moment we use.

Fig. 6 shows the MSE$_n$ results at small scales. Since the complexities at small scales (1-20) are dominated by the appearing of the high frequency rhythms, it is no surprise that the Awake stage (dominated by the alpha waves or higher frequencies) is the most complex one compared to the others. Similarly, the emergence of the stronger slow waves (from N1 to N3) can lead to a decrease in complexity. Compared to MSE$_\mu$, MSE$_{\sigma 2}$ and MSE$_{Skew}$ are more capable of distinguishing the differences in entropy between different stages. The most misleading part of MSE$_\mu$ can be the scales from 15 to 20, entropy measures converge and show fewer differences; in some extreme cases (subject 2; Fig. 6(D)), N1 can even surpass the

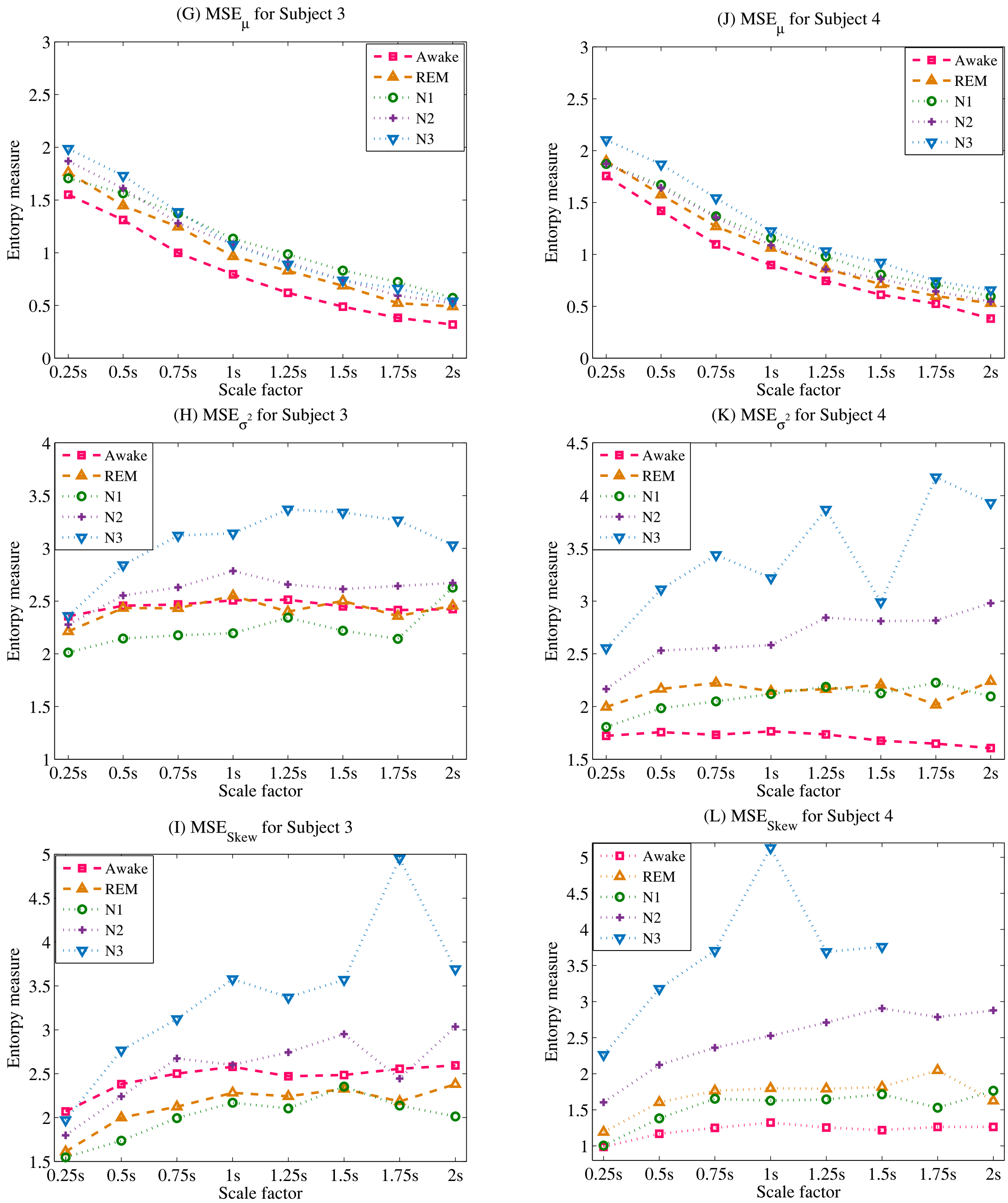

Fig. 7. Continued

Awake (crossover at scale 8). Unlike MSE$_{\mu}$, the order in different stages in entropy values at small scales is consistent using MSE$_{\sigma^2}$ and MSE$_{Skew}$. Note that the REM sleep is unique from the N-REM sleep, it has no specific position in the entropy measure using MSE$_{n}$.

Unlike the small scales (1-20) that emphasize the frequency ($>$ 25.6 Hz) of beta waves and above, it is a necessity to understand the performances at scales of delta wave ($<$4 Hz). The reason lies on the fact that nearly 50% of the epochs of N3 sleep EEG record are dominated by the frequencies of 2 Hz and slower. In our study, time scales ranged from 0.25 s and 2 s with step equal to 0.25 s are analyzed carefully to cover up the whole delta wave, which is the most significant frequency during the deep sleep as well. In Fig. 7, the order of the five sleep stages is opposite to the results in Fig. 6 in general. That is, the deep sleep or the dominance of slow waves will share the higher entropy values (N3 $>$ N2 $>$ N1). The entropy measures using MSE$_{\sigma^2}$ and MSE$_{Skew}$ faithfully and clearly manifest the above mentioned physiological concept. Regardless of the fluctuation during the Awake stages due to the enlargement value by the higher moment approaches, it will not affect the prediction of the stage orders in entropy measure. In contrast, MSE_{μ} (Fig. 7(A), (D), (G), (J)) cannot discern the differences between stages as much good as the MSE with higher moments. On the other side, the frequency of the REM sleep (2–7 Hz) is close to N1 sleep but with judgement from the emergence of rapid eye movement as well. Only the approach of MSE_{σ^2} and MSE_{Skew} can manifest the concept, that is, the REM stages (orange line) are close to the N1 stages (green line) in large scales (0.25 s–2 s).

4. Conclusion

In our present study, we extend the multiscale entropy (MSE) method using higher moments (variance and skewness) to coarse-grain a time series. We hypothesize that the increasing differences in the coarse-grained time series using MSE_{σ^2} (variance) and MSE_{Skew} (skewness) can discern the slightly differences between complex oscillations more easily. We first use the logistic map to prove the effectiveness of MSE_{σ^2} and MSE_{Skew} in predicting the complexities (chaotic) of an oscillation with the comparison to MSE_{μ}. In the application to the real sleep EEG signals, both MSE_{σ^2} and MSE_{Skew} can guarantee a stable fluctuation in entropy measures and superior discriminated abilities in the sleep stages that compared to MSE_{μ}. Our study shows that MSE_{σ^2} and MSE_{Skew} can better manifest the physiological concepts as well, that is, the entropy measures are higher in the Awake stage and lower in deep sleep (N3) at small scales (>25.6 Hz); in contrast, the measures will be lower in the Awake stage and higher in deep sleep stages at large scales (delta wave).

Acknowledgements

We gratefully acknowledge the financial supports that include the funds of the China National Science (61371130), the Beijing National Science (4162047) and China Postdoctoral Science Foundation (2015M580040).

References

[1] Hobson JA, Spagna T, Malenka R. Ethology of sleep studied with time-lapse photography: postural immobility and sleep-cycle phase in humans. Science 1978;201:1251–3.
[2] Sleep A. Technical note automatic sleep/wake identification from wrist activity. Sleep 1992;15:461–9.
[3] Redmond DP, Hegge FW. Observations on the design and specification of a wrist-worn human activity monitoring system, behavior research methods. Instr Comput 1985;17:659–69.
[4] Buysse DJ, Reynolds CF, Monk TH, Berman SR, Kupfer DJ. The pittsburgh sleep quality index: a new instrument for psychiatric practice and research. Psychiatry Res 1989;28:193–213.
[5] Johns MW. A new method for measuring daytime sleepiness: the epworth sleepiness scale. Sleep 1991;14(6):540–5.
[6] Fraiwan L, Lweesy K, Khasawneh N, Wenz H, Dickhaus H. Automated sleep stage identification system based on time-frequency analysis of a single EEG channel and random forest classifier. Comput Methods Prog Biomed 2012;108:10–19.
[7] Sen B, Peker M. Novel approaches for automated epileptic diagnosis using FCBF selection and classification algorithms. Turkish J Electr Eng Comput Sci 2013;21:2092–109.
[8] Rechtschaffen A, Kales A. A Manual of standardized terminology, techniques and scoring system for sleep stages of human subjects. Public Health Service, U.S. Goverment Priting Office; 1968.
[9] Ebrahimi F, Mikaeili M, Estrada E, Nazeran H. Automatic sleep stage classification based on EEG signals by using neural networks and wavelet packet coefficients. In: 2008 30th Annual International Conference of the IEEE Engineering in Medicine and Biology Society. IEEE; 2008. p. 1151–4.
[10] Lee JM, Kim DJ, Kim IY, Park KS, Kim SI. Detrended fluctuation analysis of EEG in sleep apnea using MIT/BIH polysomnography data. Comput Biol Med 2002;32(1):37–47.
[11] Acharya R, Faust O, Kannathal N, Chua T, Laxminarayan S. Non-linear analysis of EEG signals at various sleep stages. Comput Methods Prog Biomed 2005;80(1):37–45.
[12] Chai TY, Woo S, Rizon M, Tan CS. Classification of human emotions from EEG signals using statistical features and neural network. Int J Integr Eng 2010;1:1–6.
[13] Aeschbach D, Borély AA. All-night dynamics of the human sleep EEG. J Sleep Res 1993;2:70–81.
[14] Kannathal N, Choo ML, Acharya UR, Sadasivan PK. Entropies for detection of epilepsy in EEG. Comput Methods Prog Biomed 2005;80:187–94.
[15] Heisz JJ, McIntosh AR. Applications of EEG neuroimaging data: event-related potentials, spectral power, and multiscale entropy. J Visual Exp 2013;76.
[16] Alessandro MD, Vachtsevanos G, Hinson A, Esteller R, Echauz J, Litt B. A genetic approach to selecting the optimal feature for epileptic seizure prediction. Eng Med Biol Soc IEEE 2001;2:1703–6.
[17] Bruzzo AA, Gesierich B, Santi M, Tassinari CA, Birbaumer N, Ruboli G. Permutation entropy to detect vigilance changes and preictal states from scalp EEG in epileptic patients, a preliminary study. Neurol Sci 2008;29:3–9.
[18] Richman JS, Moorman JR. Physiological time series analysis using approximate entropy and sample entropy. Am J Physiol Heart Circ Physiol 2000;278(6):H2039–49.
[19] Shi WB, Shang PJ. Cross-sample entropy statistic as a measure of synchronism and cross-correlation of stock markets. Nonlinear Dyn 2013;71:39–554.
[20] Costa M, Goldberger AL, Peng CK. Multiscale entropy analysis of complex physiologic time series. Phys Rev Lett 2002;89:068102.
[21] Ni L, Cao JT, Wang RB. Dynamic multivariate multiscale entropy based analysis on brain death diagnosis. Sci China Technol Sci 2015;58:425–33.
[22] Bell IR, Howerter A, Jackson N, Mikel A, Bootzin RR, Brooks AJ. Nonlinear dynamical systems effects of homeopathic remedies on multiscale entropy and correlation dimension of slow wave sleep EEG in young adults with histories of coffee-induced insomnia. Homeopathy 2012;101:182–92.
[23] Costa MD, Goldberger AL. Generalized multiscale entropy analysis: application to quantifying the complex volatility of human heartbeat time series. Entropy 2015;17:1197–203.
[24] Ramdani S, Seigle B, Lagarde J, Bouchara F, Bernard PL. On the use of sample entropy to analyze human postural sway data. Med Eng Phys 2009;31:1023–31.
[25] Papoulis A. Probability, Random Variables, and Stochastic Processes. 2nd ed. New York: McGraw-Hill; 1984.
[26] Kendall MG. The derivation of multivariate sampling formulae from univariate formulae by symbolic operation. Ann Eugenics 1940;10(1):392–402.
[27] Lake DE, Richman JS, Griffin MP, Moorman JR. Sample entropy analysis of neonatal heart rate variability. Am J Physiol Regul Integr Comp Physiol 2002;283:789–97.
[28] Bandt C, Pompe B. Permutation entropy: a natural complexity measure for time series. Phys Rev Lett 2002;88:174102.
[29] Pincus SM. Approximate entropy as a measure of system complexity. Proc Natl Acad Sci U S A 1991;88:2297–301.
[30] Chon KH, Scully CG, Lu S. Approximate entropy for all signals, engineering in medicine and biology magazine. IEEE 2009;28(6):18–23.

[31] Riihijärvi J, Wellens M, Mähönen P. Measuring complexity and predictability in networks with multiscale entropy analysis. In: INFOCOM. IEEE; 2009. p. 1107–15.
[32] Costa M, Goldberger AL, Peng CK. Multiscale entropy analysis of biological signals. Phys Rev E 2005;71:021906.
[33] Carskadon MA, Dement WC. Normal human sleep: an overview. In: Kryger MH, editor. Principles and Practice of Sleep Medicine. Philidelphis: W.B. Saunders Co; 1994. p. 16–25.